RELATIONS BETWEEN LIQUEFACTION RESISTANCE AND SHEAR WAVE VELOCITY AS AFFECTED BY AGING OF SAND DEPOSITS

Roozbeh SAFAEIAN AMOLY
PhD Candidate, Civil Eng. Dept. of Eastern Mediterranean University,
Famagusta, Mersin 10, Turkey
safaeian.amoly@students.emu.edu.tr

Kenji ISHIHARA
Professor, Research and Development Initiative of Chou University, Tokyo, Japan
Kenji-ishihara@e-mail.jp

Huriye BILSEL
Associate Professor, Civil Eng. Dept. of Eastern Mediterranean University, Famagusta, Mersin 10, Turkey
huriye.bilsel@emu.edu.tr

Keywords: Aging Effect, Liquefaction Resistance, Shear Wave Velocity, Cyclic Yield Strain

ABSTRACT

Since the shear wave velocity is determined by non-destructive experiments in the narrow range of small strain, some researchers cast doubt on the assessment of medium-to-large phenomenon, i.e. liquefaction, by means of it. However, some researchers confirm that the shear wave velocity is more likely to suit for distinguishing the liquefaction and non-liquefaction susceptibility of sand deposits by means of the chart determined the correlation between the liquefaction resistance and shear wave velocity, similar to the other types of indices, i.e. SPT and CPT, in spite of its few limitations. On the other hand, such liquefaction chart has been proposed based on the liquefaction resistance of young Holocene deposits, without taking account of "age". In attempt to bridge the gap between those ideas, relations between liquefaction resistance and shear wave velocity of sand deposits are proposed under aging effect using a new-introduced index property, i.e. "cyclic reference strain" or "cyclic yield strain", which is to differentiate between new and old sand deposits. That is, the smaller the cyclic yield strain, the less ductile response of soil and vice versa. It may be concluded, therefore, that this parameter can be employed as a criterion for taking into account the cementation or the effect of age in sandy soils.

INTRODUCTION

Youd and Hoose (1977) and Youd and Perkins (1978), the first pioneers recognized that the liquefaction resistance of sandy deposits increases noticeably with geological age, indicated that the older sediments belonged to Pre-Pleistocene and Pleistocene epoch are essentially more resistant to liquefaction than the younger sediments belonged to Holocene epoch. Seed (1979) pointed out that the liquefaction resistance of undisturbed specimens extracted from a fill deposited during 1000 years over that of freshly deposited specimens of the same sand increases approximately 50-100%. Kokusho et al. (1983) observed that the cyclic strength resistance of undisturbed Narita sand relative to the cyclic resistance of freshly reconstituted laboratory samples reaches up to 80%. Troncoso et al. (1988) reported on the order of 200-350% gain in cyclic resistance of undisturbed sandy specimens, obtained from two tailings dam locations at El Cobre in Chile with various ages of 1, 5, 30 years, relative to freshly deposited specimen in laboratory. It

should be noted that the preceding studies had not been considered the aging effect along with any soil indices such as shear wave velocity.

On the other hand, the empirical correlation between the liquefaction resistance and shear wave velocity as in-situ index, which is presented by Andrus and Stokoe (2000), is based on the liquefaction of sandy deposits dating back to young Holocene epoch. The empirical correlation has been developed by many researchers such as Kayen et al. (2004), Zhou and Chen (2007), Baxter et al. (2008) and Kayen et al. (2013), without any particular consideration of the age of deposits in which experiments were carried out.

The principal aim of this paper is to propose a new procedure which takes into account the relation between liquefaction resistance and shear wave velocity as well as aging effect at the same time. As such, "cyclic yield strain" or "cyclic reference strain" is introduced as a factor may reflect upon the effect of aging on sandy deposits in order to identify new or liquefied deposits as well as un-liquefied old deposits in the same chart.

THE CONCEPT OF "CYCLIC YIELD STRAIN" OR "CYCLIC REFERENCE STRAIN"

To measure the liquefaction resistance of sandy soil, the cyclic triaxial experiments are conducted a few times (2-4 times) by various cyclic stress ratio, $R_L = \sigma_d / (2\sigma_0)$, where σ_d and σ_0 denote a single amplitude of axial stress, and initial confining stress, respectively. It is supposed that one of the cyclic stress ratios is $R_L=0.2$, which is utilized as illustrated in Figure 1(a), in order to obtain different values of single amplitude of axial strain, ε_a. After similar experiments are repeated with several cyclic stress ratios the points of same axial strain amplitude are connected to result in a set of curved lines as shown in Figure 1(a).
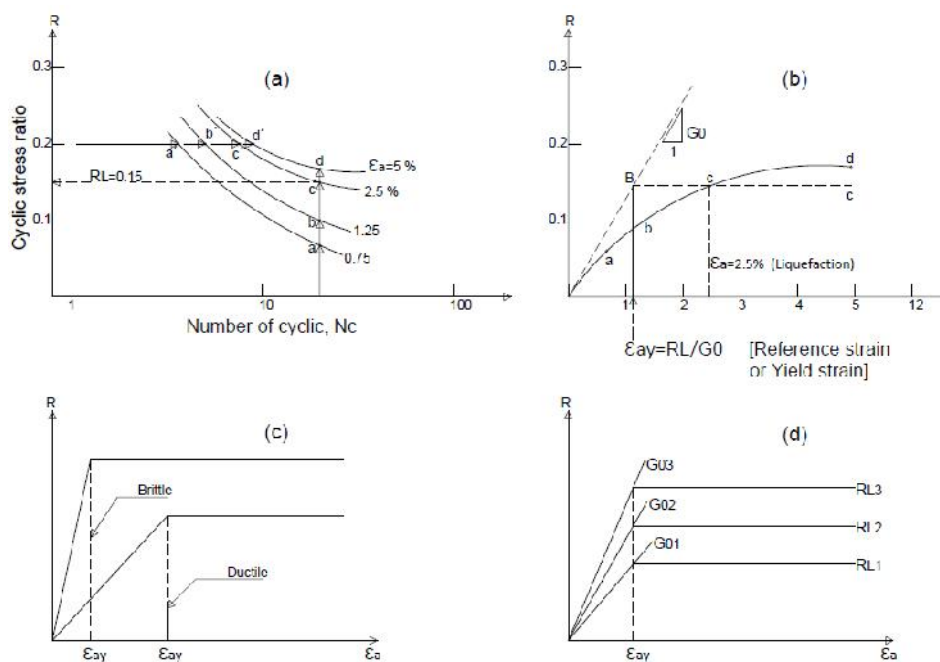

Figure 1. Schematic diagrams of the yield strain in cyclic loading (Amoly, Ishihara and Bilsel)

It should be noted that 100% pore pressure build-up occurs almost concurrently with 2.5% single amplitude of axial strain, and 10 or 20 cycles of uniformed loading can be representative of the strong earthquake with a magnitude of 7½. Thus, it has been customary to perceive the cyclic stress ratio, which is intersection of 2.5% curved line at 20 cycles, as leading liquefaction. To intersect a line perpendicular to number of cyclic axis at 20 cycles, and four curved lines, the points, i.e. a, b, c and d, are made as a function of particular cyclic stress ratio, $R_L=0.15$, as shown in Figure 1(a). Then, it is feasible to set up by connecting those points in the plot of cyclic stress ratio versus axial strain, as shown in Figure 2(b) which can generally be consider as a kind of non-linear stress-strain model.

Based on the elasto-plastic theory, bi-linear lines can approximately be representative of the non-linear stress-strain relation. As shown in Figure 1(b), elastic behavior is related to line which passes through zero point with slop, G_0, and plastic behavior is associated with the line is the level of particular cyclic stress ratio, $R_L=0.15$, the corresponding axial strain of point B, which results from intersection of two those asymptotic

lines, may be considered as a kind of "reference strain" or "yield strain" in cyclic loading. Based on Figure 1(b), cyclic yield strain, $_{ay}$, can be defined by equation 1 in order to make this strain non-dimensional format, atmospheric pressure, P_a=98 kN/m^2, multiplied by the cyclic stress ratio.

$$\varepsilon_{ay} = \frac{R_L \cdot p_a}{G_{01}} \tag{1}$$

Where, G_{01} denotes the value of G_0 at the atmospheric pressure. The physical interpretation of cyclic yield strain is shown in Figure 1(c). That is, if the value of $_{ay}$ is small, the soil is considered as a material with "brittle" behavior, which may be indicative of old aged deposits. The soil is deemed as "ductile" behavior if the value of $_{ay}$ is great, which can be representative of the new aged deposits. The level of ductility or brittleness for a particular soil could be the same if the value of $_{ay}$ remains constant as shown in Figure 1(d).

THE CORRELETION OF CYCLIC YIELD STRAIN AND SHREAR WAVE VELOCITY

Based on the dynamic property of soil, the initial shear modulus, G_0, can be derived from shear wave velocity, V_S, by equation 2. Since shear modulus at atmospheric pressure, G_{01}, is utilized in equation 1, shear wave velocity should be normalized to V_{S1} by multiplied by $(Pa/_v)^{0.25}$, where $_v$ = effective overburden pressure at particular depth, g=9.8 m/sec^2 and ρ=bulk unit weight.

$$G_{01} = \frac{\cdots}{g}V_{s1}^{\ 2} \tag{2}$$

By substituting equation 2 into equation 1 yields equation 3 which can practically be utilized in the evaluation of cyclic yield strain.

$$\vee_{ay} = \frac{R_L \cdot p_a}{G_{01}} = \frac{R_L \cdot p_a}{\cdots / g \cdot V_{s1}^{\ 2}} \tag{3}$$

UNDISTURBED SPECIMENS FOR MEASURRING CYCLIC STRAIN

To determine the value of $_{ay}$, a large number of experiments were carried out in the field as well as in the laboratory on undisturbed and disturbed specimens. For this purpose, the area of Asahi city in Chiba prefecture has been considered, which were affected by the 2011 East-Japan earthquake leading liquefaction, which is along the costal line of Pacific Ocean as shown Figure 3.

Based on geotechnical investigation, soil borings were carried out in six selected situations of that area as shown in figure 5. One of those detailed soil profiles, HG-S-1, is shown in figure 4. In order to extract undisturbed specimen, three different samplers, i.e. the thin-wall tube sampler, the triple tube sampler and the Denison sampler, are utilized based on the depth and the type of soil.

THE PROCEDURE OF CYCLIC TRIAXIAL TEST AND VS MEASUREMENT IN LABORATORY

After setting up the enclosed frozen specimens in rubber membrane, 100 mm long and 50 mm in diameter, in the chamber of cyclic traxial, it was permitted to thaw approximately 1-2 hours while employing a slight 20 kN/m^2 vacuum. Then, carbon dioxide was gradually percolated into the specimens for 30-60 minutes based on the amount of fine content. Next, the de-aired water was permitted to enter the specimens so that the B-value becomes more than 96% by applying 200 kN/m^2 back pressure. Then, let the specimens consolidated at specified effective confining pressure dependent on the depth of undisturbed specimens in soil profile. As soon as the consolidation of specimen was fully accomplished in a drained condition for approximately 30-90 minutes, it was subjected to cyclic axial load in the form of 1 Hz sinusoidal wave in un-drained condition until the axial deformation reached up to 10%. Once the cyclic loading was finalized, the

water inside the specimen was permitted to come out in order to measure the its volume change after approximately 30-60 minutes drainage.

Immediately after fully consolidation, the V_S were measured twice by means of a new device -termed "shear wave monitoring apparatus"- which is attached to the cyclic triaxial apparatus.
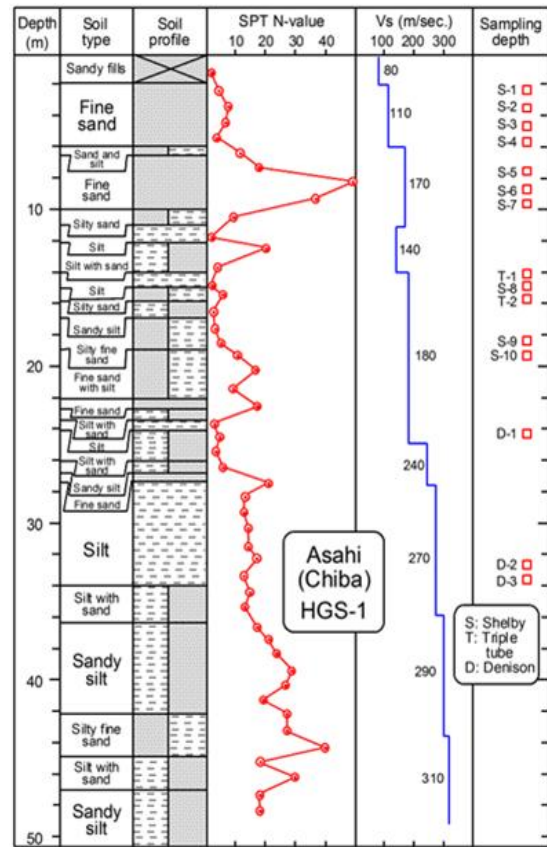

Figure 3. Situations of Asahi Site for sampling

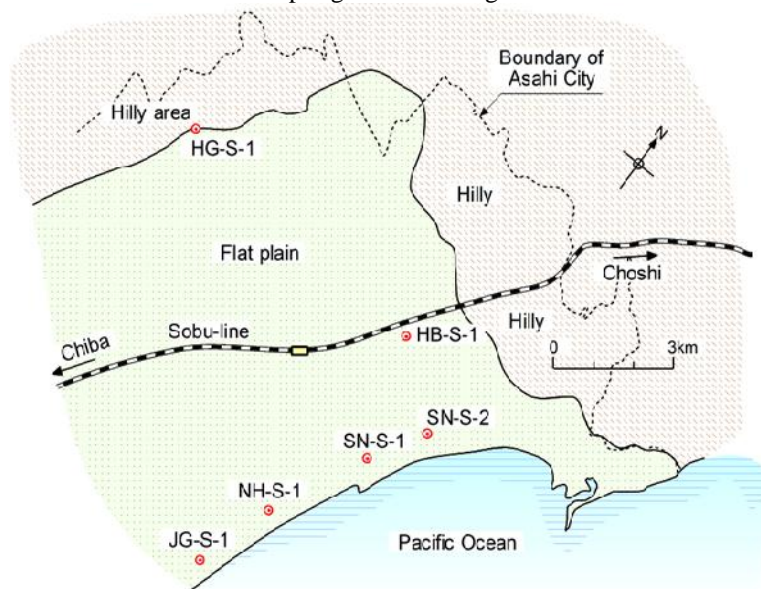Figure 4. Soil Profile from Asahi site (HG-S-1)

Figure 5. Situations of Bore Holes in Asahi Site

OUTCOMES OF EXPERIMENTS ON UNDISTURBED SPECIMENS

The outcomes of cyclic loading experiment on the undisturbed specimens from Asahi sites are indicated Table 1 and Table 2. Some of experiments were carried out by Chiba Eng. Co. without V_S

measurement in the laboratory as shown in Table. 1. Consequently, V_S values of downhole measurement are utilized. However, some other experiments were performed by Kiso-Jiban consultants Co. with cyclic triaxial apparatus equipped by a new device which can monitor shear wave velocity as shown in Table 2. In these Tables, specimens related to fills and liquefied alluviums are separated from those associated with non-liquefied alluvial and diluvial deposits. Moreover, in the column of V_{S1}, laboratory measurements of V_s are distinguished from field measurements of that by denoting "L" and "F" as laboratory and field, respectively.

THE CORRELATION BETWEEN THE CYCLIC STRENGTH AND SHEAR WAVE VELOCITY

Since new or liquefied sands are totally different from old aged sands, the correlation of cyclic strength and V_{S1} should be separated from each other. Thus, two distinctive curved lines will be proposed based on their age.

(1) The chart of cyclic strength versus V_{S1} for new age the undisturbed specimens from the new fills or liquefied sands are plotted out in Figure 5. Then, curved line as drawn through the average points in the form of $R_L = 0.9 \times 10^{-5} V_{S1}^2$, which corresponding cyclic yield strain is 4.6×10^{-6}.

(2) The chart of cyclic strength versus V_{S1} for old age the experiment data in Table 1 and 2 related to specimens from the old aged deposits denoted by D_S (Diluvial Sand) and A_S (Alluvial Sand) are plotted out in Figure 6. By drawing a curved line passing through average points of data as far as possible. The form of this curved line is $R_L = 0.68 \times 10^{-5} V_{S1}^2$, which the corresponding cyclic yield strain is 3.6×10^{-4}.

Table 1. Undisturbed Specimens from Asahi with Vs Measurement in the Field

Sampling site		Age	Depth (m)	σ'_v (kPa)	N-value	N_1-value	FC (%)	Vs (m/sec.)	V_{S1} (m/sec.)	G_{01} (MPa)	R_L	$\varepsilon_{sy} = \dfrac{R_L \cdot pa}{G_{01}}$
HB-S-1	HB-S-1 (S-1)	Fill ℓ	1.0-3.8	30	7	9	0.9	F160	L168 / F216	L52.2 / F86.3	0.304	L 5.82×10^{-4} / F 4.48×10^{-4}
	HB-S-1 (S-4)	As^n	7.0-10.9	87	25	27	1.0	F240	L189 / F248	L65.7 / F116.0	0.282	L 4.29×10^{-4} / F 2.43×10^{-4}
	HB-S-1 (S-7)	As^n	15.0-16.9	150	21	26	10.7	F190	L201 / F172	L76.4 / F55.8	0.276	L 3.61×10^{-4} / F 4.95×10^{-4}
	HB-S-1 (S-9)	As^n	22.0-23.7	215	12	8	9.6	F190	L208 / F157	L81.8 / F46.5	0.276	L 3.37×10^{-4} / F 5.94×10^{-4}
JG-S-1	JG-S-1 (S-1)	As^n	5.0-8.0	74	25	29	2.2	F180	L150 / F194	L42.9 / F71.1	0.176	L 4.10×10^{-4} / F 2.48×10^{-4}
	JG-S-1 (S-4)	As^n	8.0-9.9	91	22	23	6.6	F150	L168 / F154	L53.1 / F44.5	0.268	L 5.05×10^{-4} / F 6.02×10^{-4}
	JG-S-1 (S-6)	As^n	16.0-17.8	163	45	35	5.7	F270	L192 / F239	L69.6 / F108.0	0.280	L 4.02×10^{-4} / F 2.59×10^{-4}
	JG-S-1 (S-8)	Ds^n	26.0-27.8	248	11	7	28.7	F250	L179 / F199	L73.4 / F74.8	0.229	L 3.12×10^{-4} / F 3.06×10^{-4}
NH-S-1	NH-S-1 (S-1)	Fill ℓ	2.0-5.8	53	4	6	20.5	F140	L121 / F164	L27.3 / F50.1	0.295	L 10.8×10^{-4} / F 5.89×10^{-4}
	NH-S-1 (S-4)	As^n	10.0-11.9	112	31	30	9.6	F260	L199 / F253	L75.3 / F122.0	0.206	L 2.73×10^{-4} / F 1.69×10^{-4}
	NH-S-1 (S-6)	Ds^n	26.0-27.0	244	4	3	84.0	F150	L165 / F120	L51.4 / F27.2	0.246	L 4.78×10^{-4} / F 9.04×10^{-4}

L: Laboratory, F: Field, l: Liquefied Alluvium or Fill, n: Non-liquefied old deposits, A_s: Alluvial sand & D_s: Diluvial sand

THE CORRELATION BETWEEN LIQUEFACTION RESISTANCE AND SHEAR WAVE VELOCITY FOR NEW AND OLD AGED DEPOSITS

The curve line, in Figure 7, can be representative of old aged deposits as shown in Figure 8 along with the curve line related to new aged deposit in Figure 6. It may be concluded that the corresponding value of

new deposits, $\varepsilon_{ay} = 4.6 \times 10^{-4}$, is greater than the value of $\varepsilon_{ay} = 3.6 \times 10^{-4}$ for old deposit. This inferred, as Figure 1(c), the newly artificial deposits are associated with more of ductile feature in comparison to brittle behavior of old aged deposits.

There are several deterministic and probabilistic charts suggested for the correlation between the cyclic resistance and shear wave velocity V_{S1}. Among them, Tokimatso and Uchida (1990) and Robertson et al. (1992), Kayen et al. (2004) and Kayen et al. (2013) are highly consistent with the outcomes of this study. For instance, Kayen et al. (2004) proposed the probabilistic chart based on gathering together a global Vs data base of in-situ measurement of Vs from all over the world (Figure 9). By superimposing the two curved lines of this study on that chart, the curved line related to new deposits is placed between $P_L = 50\%$ and $P_L = 80\%$, where P_L is liquefaction potential. That is, the liquefaction susceptibly of that greater than 50% and the curved line for old deposits is placed between 20% and 50%. That is, the liquefaction susceptibility of those is less than 50% in this case, two methods of liquefaction assessment, one based on deterministic evaluation and other one based on probabilistic evaluation of in-situ measurement, are mutually confirmed in the present study as well.

CONCLUSIONS

It was indicated that the value of cyclic yield strain is directly proportional to ductile behavior of soil. That is, the more the cyclic yield strain, the higher the ductile nature of the soil. It may be concluded, therefore, that the cyclic yield strain may be a relevant parameter to take into account the age of deposits in terms of ductility or brittleness. It may also be noted that along with utilizing common correlation of cyclic strength versus shear wave velocity, the multiple curves are separately established to take account of the age of deposits.

Table 2. Undistorted Specimens from Asahi with Vs Measurement in the Laboratory

	Sampling site	Age	Depth (m)	$\sigma'v$ (kPa)	N-value	N_1-value	FC (%)	Vs (m/sec.)	V_{S1} (m/sec.)	G_{01} (MPa)	R_L	$\varepsilon_{ay} = \frac{R_L \cdot pa}{G_{01}}$
HG-S-1	HG-S-1 (S-1)	As^ℓ	2.0-3.0	25	4	6	11.8	L 127 / F 110	L 180 / F 156	L 59.5 / F 47.6	0.23	L 3.86×10^{-4} / F 4.83×10^{-4}
	HG-S-1 (S-3)	As^ℓ	4.0-5.0	60	6	8	12.1	L 115 / F 115	L 131 / F 131	L 31.5 / F 31.5	0.30	L 9.52×10^{-4} / F 9.52×10^{-4}
	HG-S-1 (S-4)	As^n	4.0-6.0	60	6	8	25.4	F 110	F 125	F 28.7	0.299	F 10.4×10^{-4}
	HG-S-1 (S-5)	As^n	7.0-10.0	87	18	19	26.2	F 170	F 176	F 45.4	0.281	F 4.80×10^{-4}
	HG-S-1 (S-9)	Ds^n	18.0-20.0	180	10	7	52.4	F 180	F 155	L 26.7 / F 45.4	0.284	F 6.25×10^{-4}
	HG-S-1 (S-9)	Ds^n	18.0-20.0	180	10	7	42.3	L 138 / F 180	L 119 / F 155	L 61.9 / F 45.4	0.28	L 10.5×10^{-4} / F 6.17×10^{-4}
SN-S-1	HG-S-1 (S-1)	$Fill^\ell$	1.0-2.0	20	5	11	1.9	L 121 / F 100	L 181 / F 149	L 61.9 / F 41.7	0.35	L 5.65×10^{-4} / F 8.39×10^{-4}
	HG-S-1 (S-10)	Ds^n	24.0-26.1	215	23	16	9.0	L 211 / F 220	L 174 / F 182	L 57.8 / F 66.3	0.24	L 4.15×10^{-4} / F 3.62×10^{-4}
SN-S-2	SN-S-2 (S-6)	As^n	13.0-14.0	115	26	24	5.0	L 209 / F 220	L 202 / F 182	L 76.3 / F 84.8	0.23	L 3.01×10^{-4} / F 2.71×10^{-4}
	SN-S-2 (S-9)	As^n	20.1-20.8	190	79	57	1.3	L 218 / F 250	L 186 / F 213	L 65.3 / F 86.4	0.22	L 3.37×10^{-4} / F 2.55×10^{-4}
	SN-S-2 (S-10)	As^n	20.8-21.8	198	79	57	5.0	L 134 / F 250	L 113 / F 211	L 24.1 / F 84.0	0.20	L 8.30×10^{-4} / F 2.38×10^{-4}

L: Laboratory, F: Field, l: Liquefied Alluvium or Fill, n: Non-liquefied old deposits, A_s: Alluvial sand & D_s: Diluvial sand
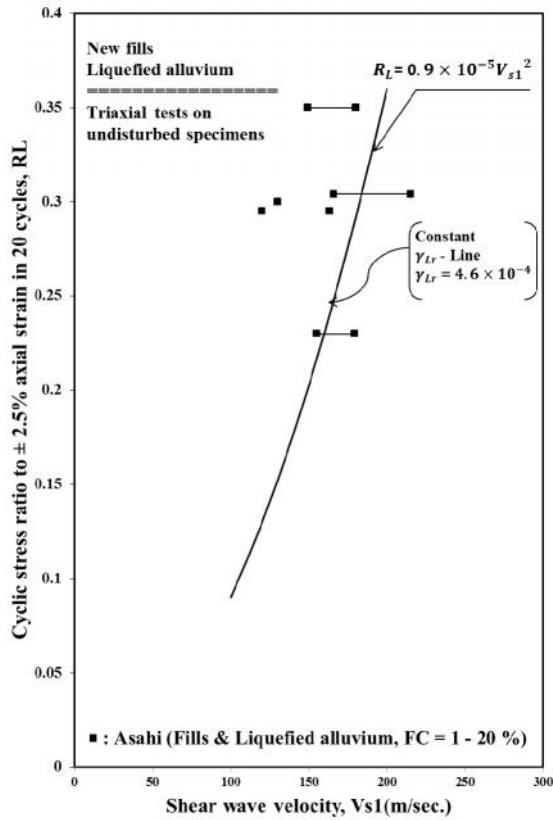
Figure 6. Correlation between the cyclic strength and shear wave velocity for intact specimens from new aged deposits.
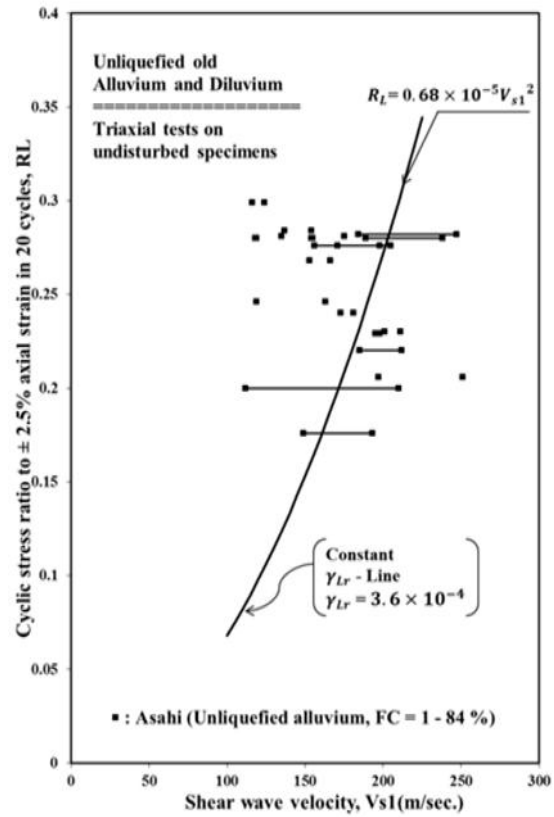

Figure 7. Correlation between the cyclic strength and shear wave velocity for intact specimens from old aged deposits.
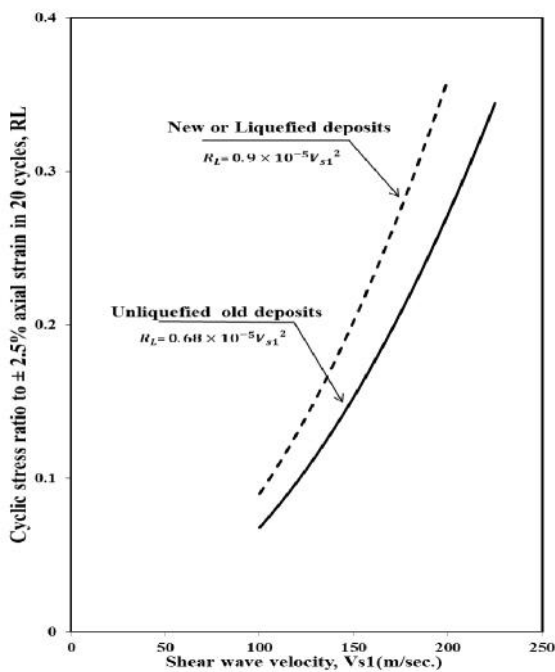

Figure 8. Two curved lines of new and old aged deposits(Amoly, Ishihara and Bilsel).
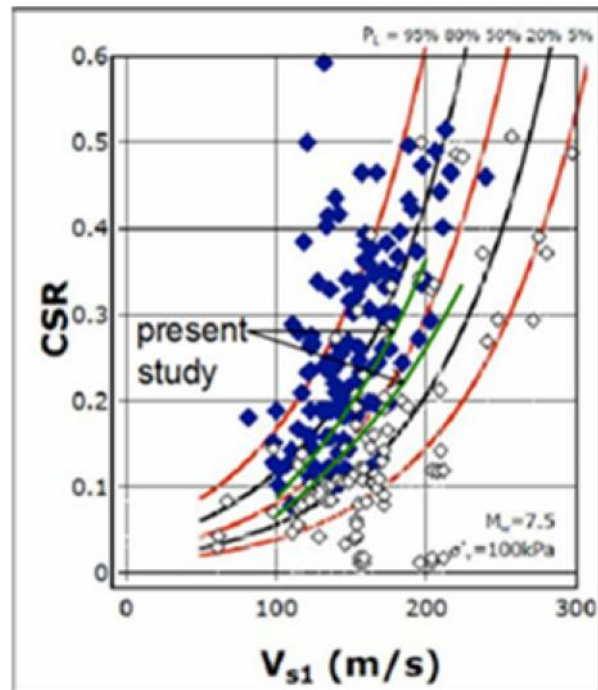

Figure 9. Curved lines of the present study along with preliminary probabilistic liquefaction onset contours determined by processing of 60% of the global V_{s1}data set to date (kayen et al., 2004).

REFERENCES

Amoly R S, Ishihara K, Belsil H (2015) Aging Effects on the Relation between Liquefaction Resistance and Shear Wave Velocity, to be submitted to Soils and Foundations, Journal of Japanese Geotechnical Society

Andrus R D and Stokoe KH II (2000) Liquefaction Resistance of Soils from Shear-Wave Velocity, Journal of Geotechnical and Geoenvironmental Engineering, ASCE, 126(11): 1015-1025

Baxter CDP, Bradshaw AS, Green RA and Wang J (2008) A New Correlation Between Cyclic Resistance and Shear Wave Velocity for Silts, Journal of Geotechnical and Geoenvironmental Engineering, ASCE, 134(1), pp. 37-46

Kayen RE, Moss RES, Thompson EM, Seed RB, Cetin KO, Der Kiureghian A, Tanaka Y and Tokimatsu K (2013) Probabilistic and Deterministic Assessment of Seismic Soil Liquefaction Potential by Shear-Wave Velocity, Journal of Geotechnical and Geoenvironmental Engineering, ASCE, Volume 139, Issue 3, March 1, pages 407-419

Kayen RE, Seed RB, Moss RES, Çetin KO, Tokimatsu K and Tanaka Y (2004a) Global Shear Wave Velocity Database for Probabilistic Assessment of the Initiation of Seismic-Soil Liquefaction, 11th International Conference on Soil Dynamics & Earthquake Engineering

Kokusho T, Yoshida Y, Nishi K and Esashi Y (1983) Evaluation of Seismic Stability of Sand Layer (part 1)," Report 383025, Electric Power Central Research Institute (In Japanese)

Robertson PK, Woeller DJ and Finn WDL (1992) Seismic Cone Penetration Test for Evaluating Liquefaction Potential under Cyclic Loading, Canadian Geotechnical Journal, Vol. 29, pp. 686-695

Troncoso J, Ishihara K, Verdugo R (1988) Aging Effects on Cyclic Shear Strength of Tailings Materials, Proceedings of Ninth World Conference on earthquake Engineering, Tokyo-Kyoto, Japan

Seed HB (1979) Soil Liquefaction and Cyclic Mobility Evaluation for Level Ground during Earthquakes, Journal of Geotechnical Engineering Division, ASCE, 105-2, 201–255

Tokimatsu K and Uchida A (1990) Correlation between Liquefaction Resistance and Shear Wave Velocity, Soils and Foundations, Journal of Japanese Geotechnical Society, Vol. 30, No. 2, pp. 33-42

Youd TL and Hoose SN (1977) Liquefaction Susceptibility and Geologic Setting, Proceedings of 6th World Conference on Earthquake Engineering, New Delhi, India, Vol. 6, 37–42

Youd TL and Perkins DM (1978) Mapping Liquefaction-induced Ground Failure Potential, Journal of Geotechnical Engineering Division, ASCE, 104, 433–446

Zhou TG and Chen TM (2007) Laboratory Investigation on Assessing Liquefaction Resistance of Sandy Soils by Shear Wave Velocity, Journal of Geotechnical and Geoenvironmental Engineering, ASCE, 133(8), 959–972